

# Characteristic orbits of charged particles around charged black holes

Aleksandra Demyanova,<sup>1,a</sup> Ozodbek Rakhimov,<sup>1,b</sup>  
Yunus Turaev,<sup>1,c</sup> Nuriddin Kurbonov<sup>1,d</sup>  
and Javlon Rayimbaev<sup>1,2,e</sup>

<sup>1</sup>Ulugh Beg Astronomical Institute, Tashkent, 100052, Uzbekistan

<sup>2</sup>National University of Uzbekistan, Tashkent 100174, Uzbekistan

<sup>a</sup>[demyanova@astrin.uz](mailto:demyanova@astrin.uz)

<sup>b</sup>[rahimov@astrin.uz](mailto:rahimov@astrin.uz) <sup>c</sup>[yunus@astrin.uz](mailto:yunus@astrin.uz)

<sup>d</sup>[nuriddin@astrin.uz](mailto:nuriddin@astrin.uz)

<sup>e</sup>[javlon@astrin.uz](mailto:javlon@astrin.uz)

## ABSTRACT

We have explored the dynamics of test particles around electrically charged Reissner-Nordström (RN) nonrotating black hole (BH). Particularly, we have studied the motion of charged particles around charged RN BH. It was found that there are two boundary conditions for specific angular momentum of stable circular orbits corresponding to innermost stable circular orbits (ISCO) and outermost stable circular orbits (OSCO). We have also shown that the accretion disk is originated between these two orbits. It was obtained the upper and lower limits for the values of the electric charge of the matter in the accretion disk around the extreme charged Reissner Nordström BH.

**Keywords:** Reissner-Nordström spacetime – black hole – test charged particle – particle dynamics – ISCO – OSCO

## 1 INTRODUCTION

Just after the discovery of general relativity two exact solutions of the Einstein field equation have been obtained by Schwarzschild describing non-rotating point-like massive object – black hole (BH) and by Reissner and Nordström independently describing the electrically and magnetically charged non-rotating black hole. However, these solutions have singularity at the center of the black hole ( $r = 0$ ), which cannot be resolved within the theory. Other electrically and magnetically charged regular black hole solutions avoiding the singularity have been obtained within the framework of general relativity coupled to non-linear electrodynamics by several authors [Bardeen \(1968\)](#); [Ayón-Beato \(1999\)](#); [Wang and Maartens \(2010\)](#).

a From astrophysical point of view the study the charged particles motion around charged BH and/or BH in external magnetic field is one of the important task. Recently, the motion of charged [Rayimbaev et al. \(2020\)](#); [Turimov et al. \(2020\)](#); [Stuchlík et al. \(2020\)](#); [Tursunov et al. \(2016\)](#), magnetized [Rayimbaev \(2016\)](#); [de Felice and Sorge \(2003\)](#); [Abdujabbarov et al. \(2020\)](#); [Vrba et al. \(2020\)](#); [Rayimbaev et al. \(2020\)](#) particles around black holes with different parameters in an external asymptotically uniform magnetic field in various theories of gravity have been studied. Particularly, the charged particle motion around Reissner-Nordström black hole has been studied in [Pugliese et al. \(2010, 2011\)](#).

In this paper we study the charged particle orbits around RN BH. The paper is organized as follow: in Sec. 2 we have considered charged particle motion in the spacetime of a charged black hole. In Sec. 3 we summarize the obtained results.

Throughout the work we use spacelike signature  $(-, +, +, +)$  for the space-time and system of units where  $G = 1 = c$ . Latin indices run from 1 to 3 and Greek ones from 0 to 3.

## 2 MOTION OF CHARGED PARTICLES AROUND REISSNER-NORDSTRÖM BLACK HOLE

The geometry of the spacetime around electrically and magnetically charged RN BH in spherical coordinates  $(x^\alpha = \{t, r, \theta, \phi\})$  is given in the following form

$$ds^2 = -fdt^2 + f^{-1}dr^2 + r^2 [d\theta^2 + \sin^2 \theta d\phi^2], \quad (1)$$

with the following gravitational metric function

$$f = 1 - \frac{2M}{r} + \frac{Q^2}{r^2}, \quad (2)$$

and associated with the four vector potential of the electromagnetic field around the electrically charged BH

$$A_\alpha = \frac{Q}{r} \{1, 0, 0, 0\}, \quad (3)$$

where  $M$  and  $Q$  are the total mass and electric charge of the RN BH, .

Here we study the charged particle with rest mass  $m$  and electric charge  $e$  around charged BH. The Lagrangian for the charged particle in the electromagnetic field in the BH environment has the following form

$$\mathcal{L} = \frac{1}{2} mg_{\mu\nu} u^\mu u^\nu + eu^\mu A_\mu. \quad (4)$$

The conserved energy and angular momentum can be found by

$$g_{tt} \dot{t} + qA_t = \mathcal{E}, \quad (5)$$

$$g_{\phi\phi} \dot{\phi} = \mathcal{L}, \quad (6)$$

where  $\mathcal{E} = E/m$  and  $\mathcal{L} = L/m$  are the specific energy and angular momentum of the particle, respectively,  $q = e/(mc)$  is the specific electric charge of the particle with mass  $m$  and electric charge  $e$ .

The equation of motion for charged particles with the Lagrangian (4) can be found using the Euler-Lagrange equation [Pugliese et al. \(2010\)](#)

$$u^\mu \nabla_\mu u^\nu = q F_{\sigma}^\nu u^\sigma, \quad (7)$$

where  $F_{\mu\sigma} = A_{\sigma,\mu} - A_{\mu,\sigma}$  is the electromagnetic field tensor. Using the equations (5-7) one may easily find the equation of motion of the charged particles at the equatorial plane ( $\theta = \pi/2$ ) in the following form:

$$\begin{aligned} \dot{t} &= \frac{1}{f} \left( \mathcal{E} - \frac{qQ}{r} \right), \\ \dot{r}^2 &= \left( \mathcal{E} - \frac{qQ}{r} \right)^2 - f \left( 1 + \frac{\mathcal{L}^2}{r^2} \right), \\ \dot{\phi} &= \frac{\mathcal{L}}{r^2}. \end{aligned} \quad (8)$$

The effective potential for charged particle in the equatorial plane (where  $\theta = \pi/2$  and  $\dot{\theta} = 0$ ) can be found solving equation  $\mathcal{E} = V_{\text{eff}}(\dot{r} = 0)$ :

$$V_{\text{eff}}^\pm(r) = \frac{qQ}{r} \pm \sqrt{f \left( 1 + \frac{\mathcal{L}^2}{r^2} \right)}. \quad (9)$$

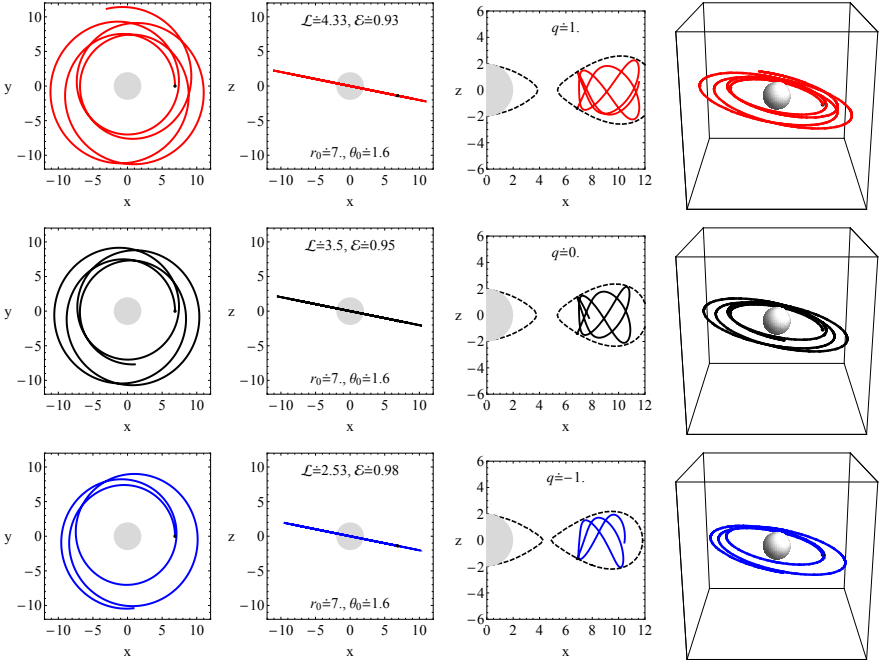
Now we will study the positive root of the effective potential  $V_{\text{eff}}^+$ : (i) In the case of  $\left| \frac{qQ}{r} \right| < \sqrt{f \left( 1 + \frac{\mathcal{L}^2}{r^2} \right)}$  the second root of the effective potential  $V_{\text{eff}}^-$  will be negative and (ii) in the case of  $\left| \frac{qQ}{r} \right| > \sqrt{f \left( 1 + \frac{\mathcal{L}^2}{r^2} \right)}$  the effective potential  $V_{\text{eff}}^-$  has neither maximum nor minimum.

Figure 1 illustrates the charged and neutral particles trajectories in similar bounded states with the same initial conditions  $r_0 = 7M$  and  $\theta_0 = 1.6$ . In this figure, the grey area implies the hypothetical surface of the BH-horizon of the BH and dashed line for the region where bounded circular orbits are allowed. Here, we have aimed to show the bounded orbits for the different (charged and neutral) particles, by changing the angular momentum of the particles. One can easily see that for the neutral particle (black solid orbits at the middle row in Fig.1) the bounded orbits exists with specific angular momentum  $\mathcal{L} = 3.5$  and energy  $\mathcal{E} = 0.95$ , while the orbits of positively charged particles  $q = 1$  are bounded for the values:  $\mathcal{L} = 4.33$  and  $\mathcal{E} = 0.93$ , and orbits of negatively charged particles  $p = 1$  are bound for the values  $\mathcal{L} = 2.53$  and  $\mathcal{E} = 0.98$  due to the different feature of Coulomb interaction.

## Stable circular orbits

Here we will study the stable circular orbits using following standard conditions

$$V_{\text{eff}} = \mathcal{E}, \quad V'_{\text{eff}} = 0, \quad V''_{\text{eff}} = 0. \quad (10)$$



**Figure 1.** Trajectories of charged particles around Reissner-Nordström black hole with  $Q = 0.5M$ .

At the equatorial plane the circular orbits can be stable for the critical value of angular momentum  $\mathcal{L}_{cr}$  which is the solution of the equation  $V'_{\text{eff}} = 0$  and have the following form:

$$\mathcal{L}_{\pm}^2 = \frac{1}{2(r(r-3M) + 2Q^2)^2} \left[ Q^2 r^3 \left( (q^2 - 2)r - 2M(q^2 - 5) \right) + 2Mr^4(r - 3M) \right. \\ \left. + (q^2 - 4)Q^4 r^2 \pm qQr^2(r(r-2M) + Q^2) \sqrt{4r(r-3M) + (q^2 + 8)Q^2} \right]. \quad (11)$$

One can see from equation (11) that for positive charges  $\mathcal{L}_+^2 < \mathcal{L}_-^2$  and for negative charges  $\mathcal{L}_-^2 > \mathcal{L}_+^2$ . We also have

$$\mathcal{L}_+^2|_{q<0} = \mathcal{L}_-^2|_{q>0} < \mathcal{L}_+^2|_{q>0} = \mathcal{L}_-^2|_{q<0}. \quad (12)$$

This can be interpreted as follow: the circular orbits exist at the values of angular momentum for positive charge with angular momentum in the range  $\mathcal{L}_-^2 \leq \mathcal{L}^2 \leq \mathcal{L}_+^2$  and negative charge with angular momentum in the range  $\mathcal{L}_-^2 \geq \mathcal{L}^2 \geq \mathcal{L}_+^2$ . The value of critical angular momentum for neutral particles ( $q = 0$ ) has the following form

$$\mathcal{L}_{\pm}^2 = \frac{r^2(Mr - Q^2)}{r(r - 3M) + 2Q^2}, \quad (13)$$

and in the case when  $Q = 0$ , we will get the Schwarzschild solution and the angular momentum takes the standard form

$$\mathcal{L}_{\pm}^2 = \frac{Mr^2}{r - 3M}. \quad (14)$$

Now we will analyze the solution (11) and look for the condition where both  $\mathcal{L}_{\pm}^2$  are real. For this we require the expression inside the square root to be non-negative:

$$(q^2 + 8)Q^2 - 4r(3M - r) \geq 0. \quad (15)$$

Thus, for the critical value of specific angular momentum  $\mathcal{L}$  we consider two cases:

Case 1 – since  $(q^2 + 8)Q^2$  is always positive, then we require the condition  $r > 3M0$  for all values of  $q$ , including neutral particles ( $q = 0$ ).

Case 2 – for the case when  $r < 3M$  we require the condition  $(q^2 + 8)Q^2 > 4r(3M - r)$  which will be satisfied for a large values of electric charge.

From the condition (15) one may get the lower limit for radius of the circular orbit of particle (at the same time the radius equals to the radius of photon circular orbits) when  $\mathcal{L}$  is still real

$$r_{\text{crit}} = \frac{3}{2}M \left( 1 + \sqrt{1 - \frac{(q^2 + 8)Q^2}{9M^2}} \right). \quad (16)$$

In expression (16), in order to have real value for  $r_{\text{crit}}$  we require the expression under the square root to be non-negative:  $9M^2 - (q^2 + 8)Q^2 \geq 0$ . This will give us the interval for the allowed values of the electric charge of the particles:

$$-\frac{\sqrt{9 - 8\frac{Q^2}{M^2}}}{Q/M} \leq q \leq \frac{\sqrt{9 - 8\frac{Q^2}{M^2}}}{Q/M}. \quad (17)$$

Expression (17) indicates the allowed value of the charge of the test particle required for circular stable orbits.

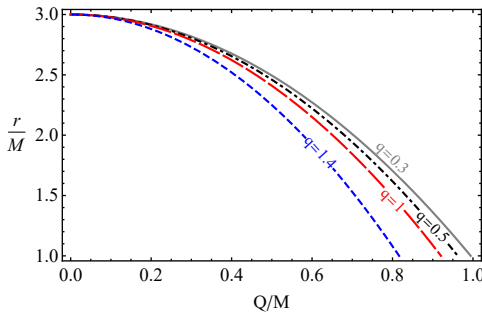


**Figure 2.** The dependence of radius of photon circular orbits on the charge of BH  $Q$  for the different values of the particle charge,  $q$ .

Figure 2 illustrates the dependence of the value of the radius of photon circular orbits from the electric charge of the BH  $Q$  for the different values of the particle charge  $q$ . One

[h]

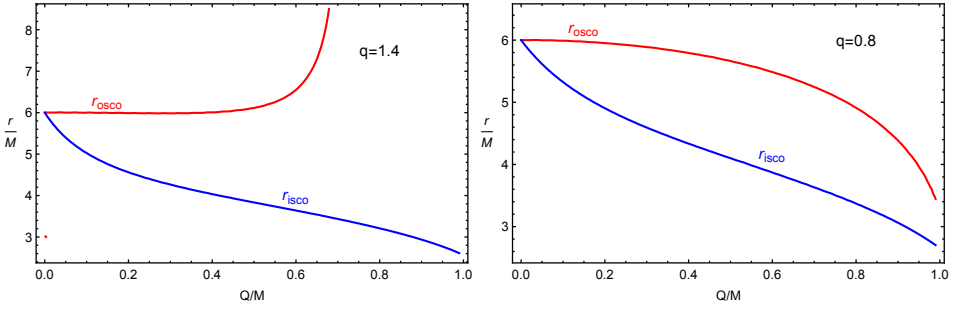


**Figure 3.** ISCO and OSCO radius as a function of black hole charge for positively charged particles.

can see that the radius decreases with the increase of the value of  $Q$ . From the Figure 2 one can also see that for the neutral test particle we get  $r_{\text{crit}} = 3M$  (the Schwarzschild case). It can be also seen from the figure that for the large values of  $Q$  and  $q$ , the photon sphere radius decreases very fast, depending both black hole and particles charge. The critical radius decreases with the increase of the black hole charge and reaches the value of  $2M$  for  $Q = M$  for neutral particle.

Now we will study the radius of stable circular orbits using the condition  $V''_{\text{eff}} \geq 0$ . There are bounds for stable circular orbits corresponding to two roots of  $\mathcal{L}^2$ . One of them called innermost stable circular orbits (ISCO) and the other one called outermost stable circular orbits (OSCO). Inner stable circular orbits requires large angular moments, while outer ones requires smaller angular momentum. Obviously, according to equation (12),  $\mathcal{L}_+^2$  for negative charges and  $\mathcal{L}_-^2$  for positively charged particles correspond to OSCO and  $\mathcal{L}_+^2$  for positively charged particles and  $\mathcal{L}_-^2$  for negatively charged particles correspond to ISCO.

Taking into account above estimations we can calculate ISCO and OSCO equations using condition for circular stable orbits (10) in the following form

$$2qQ - \frac{(r^2(\mathcal{L}_\pm^2 + Q^2) + 2\mathcal{L}_\pm^2Q^2 - Mr^3 - 3\mathcal{L}_\pm^2Mr)^2}{r(\mathcal{L}_\pm^2 + r^2)^{3/2}(r(r-2M) + Q^2)^{3/2}} + \frac{3r^2(\mathcal{L}_\pm^2 + Q^2) + 10\mathcal{L}_\pm^2Q^2 - 2Mr^3 - 12\mathcal{L}_\pm^2Mr}{r\sqrt{(\mathcal{L}_\pm^2 + r^2)[r(r-2M) + Q^2]}} \geq 0 \quad (18)$$

So, within the range  $r_{\text{isco}} \leq r \leq r_{\text{osco}}$  there is an accretion disk contains the charged particles with the different specific angular momentum.

Now, we will analyze ISCO and OSCO radius for both positively and negatively charged particles.

Figure 3 illustrates the dependence of the ISCO and OSCO radius on the charge of the RN black hole charge for positively charged particles. One can see that in both cases  $q = 1.4$  and  $q = 0.8$  ISCO radius decreases with the increase the value of black hole charge.

[h!]

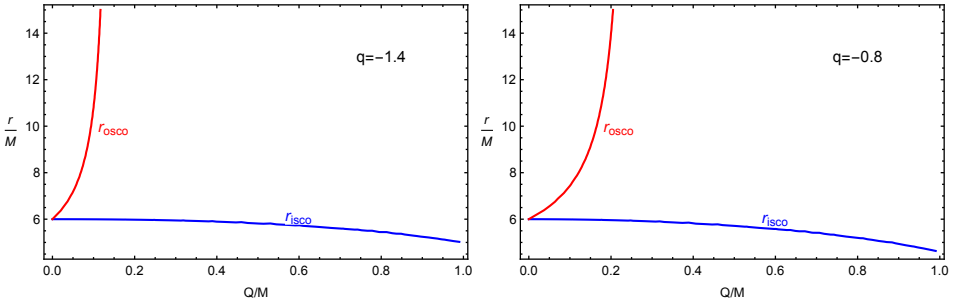


**Figure 4.** ISCO and OSCO radius as a function of black hole charge for negatively charged particles.

[h!]

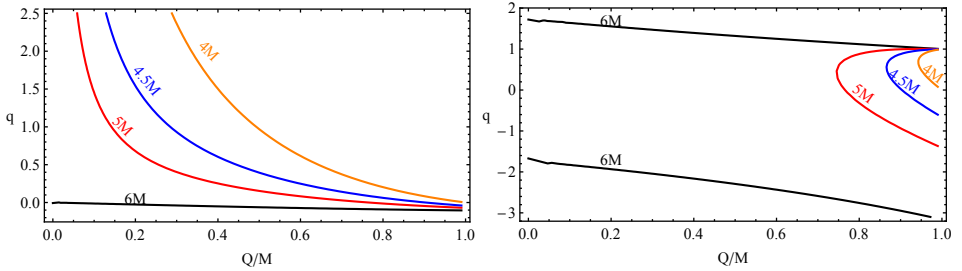


**Figure 5.**  $q - Q$  diagram for different values of ISCO (left panel) and OSCO (right panel) radius of a charged particle.

In case when  $q = 0.8$  the radius of OSCO decreases with the increase of  $Q$ , while when  $q = 1.4$  increases and tends to infinity at some upper values of  $(qQ)_{\text{upper}}$  due to domination of the Coulomb interaction.

Figure 4 illustrates the dependence of ISCO and OSCO radius on black charge for negatively charged particles. One can see that in both case  $q = -1.4$  and  $q = -0.8$  ISCO radius decreases with the increase of the value of black hole charge. The behavior of the radius of OSCO differs from the case of positive charge: for all negative charge of particles the radius of OSCO increases with the increase of the module of the charge.

In Figure 5 we present the relation between the particle's and the black hole's charges for the fixed values of ISCO and OSCO. One can see from the diagram that OSCO may not exist below the radius  $6M$  from the central object for negatively charged particles and for positively charged particles with value more than  $q = 2$ . One can also see from the right panel of the Figure 5 OSCO radius (at the range  $4M \leq r_{\text{osco}} \leq 6M$ ) can be the same for different charged particles ( $2 \leq q \leq -3$ ) for the fixed value of black hole charge.

Now we study the distance between ISCO and OSCO corresponding to the size of accretion disk  $\Delta r = r_{\text{osco}} - r_{\text{isco}}$ .

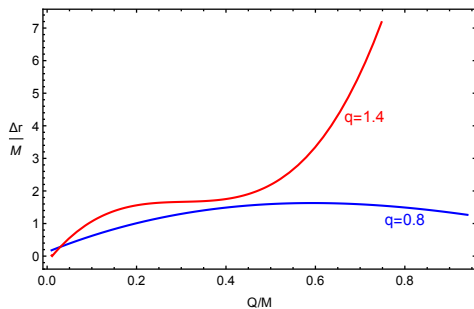


**Figure 6.** The dependence of the accretion disk size on black hole charge

In Figure 6 we show the relation between black hole charge,  $Q$ , and the size of the accretion disk which contains positively charged particles with values  $q = 0.8$  and  $q = 1.4$ . From the Figure 6 one can see that size of accretion disk for the charge with the value  $q < 1$  is always less than one in the case when  $q > 1$ . As it was shown in Figure 6 in case of when  $q = 0.8$  the size  $\Delta r$  increases with the increase of  $Q$ , reaches its maximum then starts to decrease. However, the size increases with the increase of  $Q$  up to  $\approx 0.45M$  then starts to increase due to increase the Coulomb force. Moreover, one can see that the delta  $r$  increases with increasing the particle charge. In the other words, the as sizeable specific charge of particles as wider the width of their allowed circular orbits in the accretion disk.

### 3 CONCLUSION

In this work, we have studied circular motion of charged particles around Reissner-Nordström black hole and the following main results are obtained:

- Upper and lower limits for the value of charged particle at circular orbits for the given value of RN black hole charge have been found.
- It was shown that the critical radius of circular orbits depends on particle charge.
- It was found that there are two critical values for the specific angular momentum for charged particles. One of them corresponds to the lower boundary and the other to the upper boundary of the stable circular orbits.
- It was shown that OSCO radius of positively charged particles increases with the increase of  $Q$  for  $q > 1$  and it decreases with the increase of  $Q$  for  $q < 1$ . However, OSCO radius for negatively charged particles increases with the increase of the black hole charge  $Q$ .

### ACKNOWLEDGEMENTS

This research is supported by Grants No. VA-FA-F-2-008, No. MRB-AN-2019-29 and No. YFA-Ftech-2018-8 of the Uzbekistan Ministry for Innovational Development, and by the Abdus Salam International Centre for Theoretical Physics through Grant No. OEA-NT-01.

## REFERENCES

- Abdujabbarov, A., Rayimbaev, J., Turimov, B. and Atamurotov, F. (2020), Dynamics of magnetized particles around 4-D Einstein Gauss-Bonnet black hole, *Physics of the Dark Universe*, **30**, 100715.
- Ayon-Beato, E. (1999), New regular black hole solution from nonlinear electrodynamics, *Physics Letters B*, **464**, pp. 25–29, [arXiv: hep-th/9911174](https://arxiv.org/abs/hep-th/9911174).
- Bardeen, J. (1968), in C. DeWitt and B. DeWitt, editors, *Proceedings of GR5*, p. 174, Tbilisi, USSR, Gordon and Breach.
- de Felice, F. and Sorge, F. (2003), Magnetized orbits around a Schwarzschild black hole, *Classical and Quantum Gravity*, **20**, pp. 469–481.
- Pugliese, D., Quevedo, H. and Ruffini, R. (2010), Circular motion in Reissner-Nordström spacetime, *ArXiv e-prints*, [arXiv: 1003.2687](https://arxiv.org/abs/1003.2687).
- Pugliese, D., Quevedo, H. and Ruffini, R. (2011), Motion of charged test particles in Reissner-Nordström spacetime, *Phys. Rev. D*, **83**(10), 104052, [arXiv: 1103.1807](https://arxiv.org/abs/1103.1807).
- Rayimbaev, J., Abdujabbarov, A., Jamil, M., Ahmedov, B. and Han, W.-B. (2020), Dynamics of test particles around renormalization group improved schwarzschild black holes, *Phys. Rev. D*, **102**, p. 084016, URL <https://link.aps.org/doi/10.1103/PhysRevD.102.084016>.
- Rayimbaev, J., Figueroa, M., Stuchlík, Z. and Juraev, B. (2020), Test particle orbits around regular black holes in general relativity combined with nonlinear electrodynamics, *Phys. Rev. D*, **101**(10), 104045.
- Rayimbaev, J. R. (2016), Magnetized particle motion around non-Schwarzschild black hole immersed in an external uniform magnetic field, *Astrophys Space Sc*, **361**, 288.
- Stuchlík, Z., Kološ, M., Kovář, J., Slaný, P. and Tursunov, A. (2020), Influence of Cosmic Repulsion and Magnetic Fields on Accretion Disks Rotating around Kerr Black Holes, *Universe*, **6**(2), p. 26.
- Turimov, B., Rayimbaev, J., Abdujabbarov, A., Ahmedov, B. and Stuchlík, Z. c. v. (2020), Test particle motion around a black hole in einstein-maxwell-scalar theory, *Phys. Rev. D*, **102**, p. 064052, URL <https://link.aps.org/doi/10.1103/PhysRevD.102.064052>.
- Tursunov, A., Stuchlík, Z. and Kološ, M. (2016), Circular orbits and related quasiharmonic oscillatory motion of charged particles around weakly magnetized rotating black holes, *Phys. Rev. D*, **93**(8), 084012, [arXiv: 1603.07264](https://arxiv.org/abs/1603.07264).
- Vrba, J., Abdujabbarov, A., Kološ, M., Ahmedov, B., Stuchlík, Z. and Rayimbaev, J. (2020), Charged and magnetized particles motion in the field of generic singular black holes governed by general relativity coupled to nonlinear electrodynamics, *Phys.Rev.D*, **101**(12), 124039.
- Wang, A. and Maartens, R. (2010), Cosmological perturbations in Horava-Lifshitz theory without detailed balance, *Phys. Rev. D*, **81**(2), 024009, [arXiv: 0907.1748](https://arxiv.org/abs/0907.1748).